UC Irvine
UC Irvine Previously Published Works

Title

Copper-Catalyzed Hydroamination: Enantioselective Addition of Pyrazoles to Cyclopropenes.

Authors

Wang, Minghao
Simon, Julie
Xu, Mengfei
et al.

Copper-Catalyzed Hydroamination: Enantioselective Addition of Pyrazoles to Cyclopropenes

Minghao Wang,

Department of Chemistry, University of California, Irvine, Irvine, California 92697, United States

Julie C. Simon[§],

Department of Chemistry, University of California, Irvine, Irvine, California 92697, United States

Mengfei Xu[§],

Department of Chemistry, University of California, Irvine, Irvine, California 92697, United States

Stephanie A. Corio,

Department of Chemistry, Binghamton University, Binghamton, New York 13902, United States

Jennifer S. Hirschi,

Department of Chemistry, Binghamton University, Binghamton, New York 13902, United States

Vy M. Dong

Department of Chemistry, University of California, Irvine, Irvine, California 92697, United States

Abstract

Chiral *N*-cyclopropyl pyrazoles and structurally related heterocycles are prepared using an earth-abundant copper catalyst under mild reaction conditions with high regio-, diastereo-, and enantiocontrol. The observed N^2:N^1 regioselectivity favors the more hindered nitrogen of the pyrazole. Experimental and DFT studies support a unique mechanism that features a five-centered aminocupration.

Catalytic functionalization of heterocycles presents a challenge with implications for the discovery and preparation of medcines.[1,2] Pyrazoles, a type of nitrogen-containing heterocycle,[3] rank fourth in occurrence among the most recent FDA-approved drugs (Figure 1A).[2d] Given that hydroamination is an efficient approach to form C–N bonds,[4,5] variants

Corresponding Authors: **Jennifer S. Hirschi** – Department of Chemistry, Binghamton University, Binghamton, New York 13902, United States; jhirschi@binghamton.edu, **Vy M. Dong** – Department of Chemistry, University of California, Irvine, Irvine, California 92697, United States; dongv@uci.edu.
§J.C.S. and M.X. contributed equally.

that feature nitrogen-containing heterocycles warrant development.[6] To date, pyrazoles undergo addition to allenes,[6a,c] alkynes,[6b] and dienes,[6d,e] albeit using precious metals (namely, Rh and Pd). As a promising alternative, Cu–amido complexes[7] (first isolated and characterized by Gunnoe[8a]) catalyze the addition of amines to electron-deficient olefins,[8c,d] allenes,[9b] nitrostyrenes,[9c] and azabenzonorbornadienes.[9d] Despite this reactivity, no asymmetric variants were yet achieved (Figure 1B). In this study, we report a Cu-catalyzed hydroamination with pyrazoles that provides chiral cyclopropyl motifs with high regio-, diastereo-, and enantiocontrol (Figure 1C).

The hydrofunctionalization of cyclopropenes represents a versatile strategy for accessing chiral cyclopropanes.[10–12] Most relevant to our current study, Hou and co-workers disclosed the asymmetric coupling of cyclopropenes with secondary amines (e.g., morpholine, pyrrolidine, and dibenzylamines) by using a rare-earth metal catalyst (Sm).[12d] Buchwald and co-workers developed an enantioselective hydroamination of 1-silyl- or 1-aryl-substituted cyclopropenes using Cu–H catalysis,[12h] with O-benzoylhydroxylamines as oxidants[13] and silanes as the stoichiometric reductant.[14] We hypothesized that the deprotonation of pyrazole with a catalytic amount of base would generate a Cu–pyrazolate catalyst, which would undergo aminocupration to cyclopropenes (Figure 1C).[15] Subsequent protodemetalation would produce cyclopropyl pyrazoles. If successful, this method would enable a novel and late-stage[16] cyclopropylation of pyrazoles with high atom economy.[17]

To begin this study, we focused on the desymmetrization of achiral cyclopropene **1a** with pyrazole (**2a**) to generate cyclopropyl pyrazole **3a**, which bears two stereogenic centers. An initial experiment with Cu in the absence of ligands resulted in the formation of allylic pyrazole **5a** (Figure 2A). Achiral ligands, such as *rac*-BINAP, led to the exclusive formation of the same undesired isomer **5a**, likely via a ring-opening pathway[12h,18] involving N–H bond insertion into allylic carbene **5a′**.[19] Using commercial (IPr)CuCl offered high chemoselectivity to **3a** (see the Supporting Information (SI)).[9d] However, efforts to generate chiral NHC–Cu complexes *in situ* from imidazolium salts provided **5a** more favorably; we presume that the ring-opening pathway with CuCl outcompetes NHC carbene formation and ligation. Gunnoe observed enhanced Cu–N nucleophilicity with bulky electron-rich phosphine ligands compared to NHC ligands.[8b,d] We wondered whether bulky phosphine ligands would favor Cu–amido insertion over ring opening (Figure 2B). We found that bulky chiral phosphines (**L1–L7**) gave promising results. Among them, high enantioselectivity (90:10 *er*) and yield (90%) of **3a** were observed using (*R,R*)-*i*-Pr-Duphos (**L3**). We observed improved enantioselectivity (94:6 *er*) with CH$_3$CN as the solvent (see the SI). Although lowering the temperature to 0 °C improved the enantiomeric ratio, a longer reaction time (4 days) was necessary. Therefore, we chose to explore the substrate scope at 30 °C.

With this mild protocol in hand, we evaluated the enantioselective coupling of various pyrazoles to cyclopropene **1a** (Table 1). In general, high diastereoselectivity (>20:1) was observed, likely due to the large steric difference between methyl and phenyl substituents.[20] Symmetric pyrazoles afforded **3b–3i** with high enantioselectivity (91:9–99:1 *er*) in 40–94% yield. Introducing a methyl substituent on the pyrazole showed no significant effect on reactivity (**3b**), whereas more hindered dimethylated pyrazoles gave decreased yields (**3h, 3i**). Electron-withdrawing groups on pyrazoles were accommodated (**3c–3f**), although

we observed more undesired allylic pyrazole with cyano substitution (**3e**). In the case of unsymmetric pyrazoles, 65–90% yield, 92:8–99:1 *er*, and nitrogen regioselectivity (N^2:N^1 > 20:1) were observed (**3j–3o**). X-ray crystallographic analysis of **3j** confirmed the coupling of cyclopropene with the *more* sterically hindered nitrogen of the pyrazole; this regioselectivity is rare in pyrazole functionalization.[9d,21,22] Further NOE experiments confirmed similar regiocontrol for related pyrazole substrates (see the SI). Despite the presence of a competing amino group, **3l** was isolated exclusively, showing a highly chemoselective cyclopropylation for pyrazole nitrogens.

Next, we investigated hydroamination using other heterocycles under the standard conditions. Pyridazinone (**2p**), a nitrogen-rich and medicinally relevant heterocycle,[23] provided **3p** in 55% yield, 87:13 *er*, and >20:1 nitrogen regioselectivity. Indazole, a heterocycle used as an indole bioisostere,[24] showed promising results. Chiral indazoles (**3q–3t**) were prepared in up to 66% yield with 89:11–92:8 *er* and nitrogen regioselectivity (3.1:1 to >20:1 *rr*).[25] The coupling of **1a** with indazoles required higher temperatures and resulted in lower regioselectivity, except for electron-withdrawing ester substitution (**3t**). Other nitrogen nucleophiles, such as imidazole, triazole, and aniline, exhibited no desired reactivity under standard conditions and warrant further development.[9a]

In addition, we studied the enantioselective hydroamination of pyrazole **2a** with various cyclopropenes **1** (Table 2). The electronic properties of the phenyl ring on **1** have a negligible impact on the enantioselectivity and reactivity. Good yields (60–89%) and enantioselectivity (92:8–94:6 *er*) were observed with both electron-rich (**4b**, **4c**, **4f**, and **4g**) and electron-deficient (**4d**, **4e**) substrates. Replacing the phenyl ring on **1** with other aromatic rings afforded the desired results. Both thiophenyl- (**1h**) and naphthyl-substituted (**1i**) cyclopropenes resulted in high yields (74 and 96%, respectively) and enantioselectivities (93:7 *er*). The absolute configuration of compound **4i** was confirmed by X-ray crystallographic analysis. An enhancement in enantioselectivity was observed with the incorporation of a methoxy substituent (**1j**, 96:4 *er*) or an amide substituent (**1k**, 99:1 *er*) on the cyclopropene. X-ray crystallographic analysis of **4k** suggested a potential directing group effect because pyrazole added *cis* to the amide substituent.[12a] Cyclopropenes with a spirocycle (**1l**) and an ethyl substituent (**1m**) both exhibited high reactivity (63–80%) and enantioselectivity (94:6–95:5 *er*). Furthermore, a dialkyl-substituted cyclopropene (**1n**) provided product **4n** in 80% yield with 89:11 *er*, although as a 1:1 mixture of diastereomers.[12c,d,i]

On the basis of our own observations and literature precedent, we propose a mechanism for this Cu-catalyzed hydroamination (Figure 3). The catalyst resting state is inactive off-cycle copper dipyrazolate **V**. Dissociation of one pyrazolate releases active copper–amido catalyst **I**, which enters the catalytic cycle and binds to cyclopropene **1a**. A subsequent *cis*-aminocupration of π complex **II** forges the key C–N bond and provides cyclopropylcopper intermediate III.[12e,15] Protodemetalation of **III** with DBU–H^+ affords copper complex **IV**,[26] which then undergoes ligand exchange with pyrazole **2a** to restart the catalytic cycle. Mechanistic studies that led to the proposed mechanism are discussed below.

To probe the mechanism, we studied the kinetic profile using variable-time normalization analysis (VTNA) (see the SI).[27] We observed a first-order dependence on both cyclopropene (**1a**) and the copper catalyst. We found an inverse-first-order dependence on pyrazole (**2a**), and a fractional order (0.5) for DBU. Our lab has previously identified negative fractional orders of thiols in Rh-catalyzed hydrothiolations, which we attributed to the coordination of multiple thiols to an off-cycle catalyst resting state.[12g,28] Given the coordinating ability of pyrazoles, we propose that pyrazole (**1a**) is involved in the formation of the off-cycle copper resting state with a 2:1 relative ratio of pyrazole per copper center. In the Heck coupling, Blackmond and co-workers observed that the order in Pd catalyst varied between first order and fractional order (0.5), depending on the amount of catalyst monomer released from an off-cycle dimer.[29] By performing VTNA at higher copper loadings, we observed an apparent fractional order (0.5) in copper (Figure 4A), which suggests the possibility of a Cu dimer off-cycle resting state.[30]

We then performed ^{31}P NMR studies to study the catalyst resting state (see the SI). Through monitoring the chemical shift of **L3** in the reaction of cyclopropene **1a** with pyrazole **2a**, we identified a plausible catalyst resting state at –2.4 ppm, which was replaced by another species bearing a singlet at –4.7 ppm when the transformation was near completion. NMR titrations[31] using stoichiometric catalyst, DBU, and pyrazole suggest the former resonance to be a Cu–Duphos–pyrazolate species[32] and the latter to be a Cu–Duphos–DBU complex. These NMR studies provide evidence for the dual role of DBU, acting as a base to deprotonate the pyrazole and as a ligand to copper.[26] The apparent fractional order of DBU may arise from its multiple roles in proton transfer and ligation.

Efforts to characterize the resting state under high copper concentrations led us to the serendipitous observation of trimeric copper species **VI**. X-ray crystallographic analysis revealed the unique structure where the central copper bridges two neighboring Cu–Duphos complexes via four pyrazolates (Figure 4B). The reactivity of this crystal was then tested under otherwise standard conditions, where the desired product was isolated in 20% yield with 94:6 *er*. Due to an unexpected partial oxidation during crystallization, the central copper appears divalent, which accounts for the lowered reactivity. The structure of **VI** supports the feasibility of copper–pyrazolates.[32]

A deuterium labeling experiment was conducted under the standard conditions using deuterated cyclopropene *d*-**1a** and indazole **2q** (Figure 4C). Analysis of *d*-**3q** shows exclusively *syn* proton incorporation relative to indazole. The results support the idea that C–N bond formation is an inner-sphere *cis*-aminocupration, as opposed to an outer-sphere nucleophilic addition,[7e] followed by a retentive protodemetalation.

Although a four-centered 1,2-migratory insertion of cyclopropene into the Cu–N bond was initially envisioned, the N^2:N^1 regioselectivity observed suggests that aminocupration may occur via a $1',6'$-migratory insertion (Figure 5A). In the proposed five-centered mechanism,[33] the less-hindered nitrogen (N^1) coordinates with copper, and the C–N bond is forged between the cyclopropane and the more-hindered nitrogen atom (N^2). Moreover, this mechanistic rationale is in line with Lee's observations on pyrazole hydroamination.[9d]

To explore the unique regioselectivity, we performed a density functional theory (DFT) analysis of the Cu–**L3**-catalyzed coupling of cyclopropene **1a** and pyrazole **2j** to yield **3j**. DFT calculations were performed at the M06–2X/6–311+G** PCM(MeCN)//M06–2X/ 6–31G* level of theory,[34–36] as implemented in Gaussian 16.[37] The transition structures (TSs) for aminocupration, namely, the five-centered TS versus the four-centered TS, were pursued for formation of both the N^2 and N^1 isomers of **3j** (Figure 5B). We discovered that the five-centered aminocupration leading to addition at N^2 represents the lowest-energy TS (Figure 5B, **TS$_{CA-N2}$**). This favorable transition structure (**TS$_{CA-N2}$**) has a C–Cu bond forming at 2.22 Å, a C–N bond occurring at 2.31 Å, and a Cu–N bond remaining intact at 1.99 Å. An analogous TS leading to the minor N^1 regioisomer shows the coordination of N^2 to copper and C–N bond formation from N^1 (**TS$_{CA-N1}$**); this pathway is 2.7 kcal/mol higher in energy than **TS$_{CA-N2}$**. These predictions are consistent with the experimentally observed N^2:N^1 regioselectivity. Finally, addition of pyrazole **2j** into cyclopropane **1a** via a 1,2-migratory insertion mechanism is disfavored for the TSs leading to both regioisomers of **3j**; the TSs for insertion of N^1 and N^2 (**TS$_{MI-N1}$** and **TS$_{MI-N2}$**) are higher in energy than **TS$_{CA-N2}$** by 13.6 and 16.1 kcal/mol, respectively.

In summary, hydroamination presents an attractive approach for the enantioselective coupling of cyclopropenes and pyrazoles. Chiral *N*-cyclopropyl pyrazoles and structurally related heterocycles are prepared using an earth-abundant copper catalyst under mild reaction conditions with high regio-, diastereo-, and enantiocontrol. Mechanistic studies suggest a unique 1′,6′-migratory insertion. This Cu–amido strategy complements the Cu–hydride approach to hydroamination and will guide future studies of N-heterocycle functionalization.

Supplementary Material

Refer to Web version on PubMed Central for supplementary material.

ACKNOWLEDGMENTS

REFERENCES

(1). Ertl P; Schuhmann T A Systematic Cheminformatics Analysis of Functional Groups Occurring in Natural Products. J. Nat. Prod 2019, 82, 1258–1263. [PubMed: 30933507]

(2). For reviews, see:(a)Vitaku E; Smith DT; Njardarson JT Analysis of the Structural Diversity, Substitution Patterns, and Frequency of Nitrogen Heterocycles among U.S. FDA Approved Pharmaceuticals: Miniperspective. J. Med. Chem 2014, 57, 10257–10274. [PubMed: 25255204] (b)Kalaria PN; Karad SC; Raval DK A Review on Diverse Heterocyclic Compounds as the Privileged Scaffolds in Antimalarial Drug Discovery. Eur. J. Med. Chem 2018, 158, 917– 936. [PubMed: 30261467] (c)Kerru N; Gummidi L; Maddila S; Gangu KK; Jonnalagadda SB A Review on Recent Advances in Nitrogen-Containing Molecules and Their Biological Applications. Molecules 2020, 25, 1909. [PubMed: 32326131] (d)Bhutani P; Joshi G; Raja

N; Bachhav N; Rajanna PK; Bhutani H; Paul AT; Kumar R U.S. FDA Approved Drugs from 2015-June 2020: A Perspective. J. Med. Chem 2021, 64, 2339–2381. [PubMed: 33617716]

(3). Karrouchi K; Radi S; Ramli Y; Taoufik J; Mabkhot Y; Alaizari F; Ansar M Synthesis and Pharmacological Activities of Pyrazole Derivatives: A Review. Molecules 2018, 23, 134. [PubMed: 29329257]

(4). For reviews, see:(a)Beller M; Seayad J; Tillack A; Jiao H Catalytic Markovnikov and Anti-Markovnikov Functionalization of Alkenes and Alkynes: Recent Developments and Trends. Angew. Chem., Int. Ed 2004, 43, 3368–3398.(b)Mülsler TE; Hultzsch KC; Yus M; Foubelo F; Tada M Hydroamination: Direct Addition of Amines to Alkenes and Alkynes. Chem. Rev 2008, 108, 3795–3892. [PubMed: 18729420] (c)Huang L; Arndt M; Gooßen K; Heydt H; Gooßen LJ Late Transition Metal-Catalyzed Hydroamination and Hydroamidation. Chem. Rev 2015, 115, 2596–2697. [PubMed: 25721762] (d)Colonna P; Bezzenine S; Gil R; Hannedouche J Alkene Hydroamination via Earth-Abundant Transition Metal (Iron, Cobalt, Copper and Zinc) Catalysis: A Mechanistic Overview. Adv. Synth. Catal 2020, 362, 1550–1563.

(5). For selected examples of recent hydroamination, see:(a)Pronin SV; Tabor MG; Jansen DJ; Shenvi RA A Stereoselective Hydroamination Transform To Access Polysubstituted Indolizidines. J. Am. Chem. Soc 2012, 134, 2012–2015. [PubMed: 22263967] (b)Yang Y; Shi S-L; Niu D; Liu P; Buchwald SL Catalytic Asymmetric Hydroamination of Unactivated Internal Olefins to Aliphatic Amines. Science 2015, 349, 62–66. [PubMed: 26138973] (c)Gurak JA; Yang KS; Liu Z; Engle KM Directed, Regiocontrolled Hydroamination of Unactivated Alkenes via Proto-depalladation. J. Am. Chem. Soc 2016, 138, 5805–5808. [PubMed: 27093112] (d)Musacchio AJ; Lainhart BC; Zhang X; Naguib SG; Sherwood TC; Knowles RR Catalytic Intermolecular Hydroaminations of Unactivated Olefins with Secondary Alkyl Amines. Science 2017, 355, 727–730. [PubMed: 28209894] (e)Xi Y; Ma S; Hartwig JF Catalytic Asymmetric Addition of an Amine N-H Bond across Internal Alkenes. Nature 2020, 588, 254–260. [PubMed: 33142305] (f)Chinn AJ; Sedillo K; Doyle AG Phosphine/Photoredox Catalyzed Anti-Markovnikov Hydroamination of Olefins with Primary Sulfonamides via a-Scission from Phosphoranyl Radicals. J. Am. Chem. Soc 2021, 143, 18331–18338. [PubMed: 34672192]

(6). For selected examples of hydroamination with heterocycles, see:(a)Haydl AM; Xu K; Breit B Regio- and Enantioselective Synthesis of N-Substituted Pyrazoles by Rhodium-Catalyzed Asymmetric Addition to Allenes. Angew. Chem., Int. Ed 2015, 54, 7149–7153.(b)Haydl AM; Hilpert LJ; Breit B Regioconvergent and Enantioselective Rhodium-Catalyzed Hydroamination of Internal and Terminal Alkynes: A Highly Flexible Access to Chiral Pyrazoles. Chem. - Eur. J 2016, 22, 6547–6551. [PubMed: 26990445] (c)Hilpert LJ; Sieger SV; Haydl AM; Breit B Palladium-and Rhodium-Catalyzed Dynamic Kinetic Resolution of Racemic Internal Allenes Towards Chiral Pyrazoles. Angew. Chem., Int. Ed 2019, 58, 3378–3381.(d)Jiang W; Ji D; Zhang W; Zhang G; Min X; Hu Y; Jiang X; Chen Q Orthogonal Regulation of Nucleophilic and Electrophilic Sites in Pd-Catalyzed Regiodivergent Couplings between Indazoles and Isoprene. Angew. Chem., Int. Ed 2021, 60, 8321–8328.(e)Jiu AY; Slocumb HS; Yeung CS; Yang X; Dong VM Enantioselective Addition of Pyrazoles to Dienes. Angew. Chem., Int. Ed 2021, 60, 19660–19664.

(7). For selected examples of copper–amido implicated in cross-coupling, see:(a)Strieter ER; Bhayana B; Buchwald SL Mechanistic Studies on the Copper-Catalyzed N- Arylation of Amides. J. Am. Chem. Soc 2009, 131, 78–88. [PubMed: 19072233] (b)Mankad NP; Antholine WE; Szilagyi RK; Peters JC Three-Coordinate Copper(I) Amido and Aminyl Radical Complexes. J. Am. Chem. Soc 2009, 131, 3878–3880. [PubMed: 19253942] (c)Giri R; Hartwig JF Cu(I)-Amido Complexes in the Ullmann Reaction: Reactions of Cu(I)-Amido Complexes with Iodoarenes with and without Autocatalysis by CuI. J. Am. Chem. Soc 2010, 132, 15860–15863. [PubMed: 20977264] (d)Creutz SE; Lotito KJ; Fu GC; Peters JC Photoinduced Ullmann C-N Coupling: Demonstrating the Viability of a Radical Pathway. Science 2012, 338, 647–651. [PubMed: 23118186] (e)Kainz QM; Matier CD; Bartoszewicz A; Zultanski SL; Peters JC; Fu GC Asymmetric Copper-Catalyzed C-N Cross-Couplings Induced by Visible Light. Science 2016, 351, 681–684. [PubMed: 26912852] (f)Liang Y; Zhang X; MacMillan DWC Decarboxylative sp[3] C-N Coupling via Dual Copper and Photoredox Catalysis. Nature 2018, 559, 83–88. [PubMed: 29925943] (g)Chen C; Peters JC; Fu GC Photoinduced Copper-Catalyzed Asymmetric Amidation via Ligand Cooperativity. Nature 2021, 596, 250–256. [PubMed: 34182570]

(8). For selected examples, see:(a)Blue ED; Davis A; Conner D; Gunnoe TB; Boyle PD; White PS Synthesis, Solid-State Crystal Structure, and Reactivity of a Monomeric Copper(I) Anilido Complex. J. Am. Chem. Soc 2003, 125, 9435–9441. [PubMed: 12889974] (b)Goj LA; Blue ED; Munro-Leighton C; Gunnoe TB; Petersen JL Cleavage of X-H Bonds (X = N, O, or C) by Copper(I) Alkyl Complexes To Form Monomeric Two-Coordinate Copper(I) Systems. Inorg. Chem 2005, 44, 8647–8649. [PubMed: 16296815] (c)Munro-Leighton C; Blue ED; Gunnoe TB Anti-Markovnikov N-H and O-H Additions to Electron-Deficient Olefins Catalyzed by Well-Defined Cu(I) Anilido, Ethoxide, and Phenoxide Systems. J. Am. Chem. Soc 2006, 128, 1446–1447. [PubMed: 16448104] (d)Goj LA; Blue ED; Delp SA; Gunnoe TB; Cundari TR; Pierpont AW; Petersen JL; Boyle PD Chemistry Surrounding Monomeric Copper(I) Methyl, Phenyl, Anilido, Ethoxide, and Phenoxide Complexes Supported by N -Heterocyclic Carbene Ligands: Reactivity Consistent with Both Early and Late Transition Metal Systems. Inorg. Chem 2006, 45, 9032–9045. [PubMed: 17054364]

(9). For selected examples, see:(a)Kim S; Kang S; Kim G; Lee Y Copper-Catalyzed Aza-Michael Addition of Aromatic Amines or Aromatic Aza-Heterocycles to α,β-Unsaturated Olefins. J. Org. Chem 2016, 81, 4048–4057. [PubMed: 27080327] (b)Perego LA; Blieck R; Groué A; Monnier F; Taillefer M; Ciofini I; Grimaud L Copper-Catalyzed Hydroamination of Allenes: From Mechanistic Understanding to Methodology Development. ACS Catal. 2017, 7, 4253–4264.(c)Park S; Kang S; Lee Y Copper-Catalyzed Intermolecular Hydroamination of Arylamines or Aza-Heterocycles with Nitrostyrene Derivatives. Adv. Synth. Catal 2019, 361, 1071–1083. (d)Kim K; Lee Y Copper-Catalyzed Hydroamination of Oxa- and Azabenzonorbornadienes with Pyrazoles. J. Org. Chem 2022, 87, 569–578. [PubMed: 34951305]

(10). For reviews on the importance of cyclopropane moiety in medicinal chemistry, see:(a)Talele TT The "Cyclopropyl Fragment" Is a Versatile Player That Frequently Appears in Preclinical/ Clinical Drug Molecules. J. Med. Chem 2016, 59, 8712–8756. [PubMed: 27299736] (b)Shearer J; Castro JL; Lawson ADG; MacCoss M; Taylor RD Rings in Clinical Trials and Drugs: Present and Future. J. Med. Chem 2022, 65, 8699–8712. [PubMed: 35730680]

(11). Dian L; Marek I Asymmetric Preparation of Polysubstituted Cyclopropanes Based on Direct Functionalization of Achiral Three-Membered Carbocycles: Focus Review. Chem. Rev 2018, 118, 8415–8434. [PubMed: 30156832]

(12). For selected examples of the hydrofunctionalization of cyclopropenes, see:(a)Tarwade V; Liu X; Yan N; Fox JM Directed Carbozincation Reactions of Cyclopropene Derivatives. J. Am. Chem. Soc 2009, 131, 5382–5383. [PubMed: 19323580] (b)Phan DHT; Kou KGM; Dong VM Enantioselective Desymmetrization of Cyclopropenes by Hydroacylation. J. Am. Chem. Soc 2010, 132, 16354–16355. [PubMed: 21028819] (c)Parra A; Amenós L; Guisán-Ceinos M; López A; García Ruano JL; Tortosa M Copper-Catalyzed Diastereo- and Enantioselective Desymmetrization of Cyclopropenes: Synthesis of Cyclopropylboronates. J. Am. Chem. Soc 2014, 136, 15833–15836. [PubMed: 25340304] (d)Teng H-L; Luo Y; Wang B; Zhang L; Nishiura M; Hou Z Synthesis of Chiral Aminocyclopropanes by Rare-Earth-Metal-Catalyzed Cyclopropene Hydroamination. Angew. Chem., Int. Ed 2016, 55, 15406–15410.(e)Li Z; Zhao J; Sun B; Zhou T; Liu M; Liu S; Zhang M; Zhang Q Asymmetric Nitrone Synthesis via Ligand-Enabled Copper-Catalyzed Cope-Type Hydroamination of Cyclopropene with Oxime. J. Am. Chem. Soc 2017, 139, 11702–11705. [PubMed: 28783362] (f)Dian L; Marek I Rhodium-Catalyzed Arylation of Cyclopropenes Based on Asymmetric Direct Functionalization of Three Membered Carbocycles. Angew. Chem., Int. Ed 2018, 57, 3682–3686.(g)Zhang H; Huang W; Wang T; Meng F Cobalt-Catalyzed Diastereo-and Enantioselective Hydroalkenylation of Cyclopropenes with Alkenylboronic Acids. Angew. Chem., Int. Ed 2019, 58, 11049–11053.(h)Feng S; Hao H; Liu P; Buchwald SL Diastereo- and Enantioselective CuH-Catalyzed Hydroamination of Strained Trisubstituted Alkenes. ACS Catal. 2020, 10, 282–291. [PubMed: 33664986] (i)Dian L; Marek I Pd-Catalyzed Enantioselective Hydro-alkynylation of Cyclopropenes. ACS Catal. 2020, 10, 1289–1293. [PubMed: 32953232] (j)Huang W; Meng F Cobalt-Catalyzed Diastereo- and Enantioselective Hydroalkylation of Cyclopropenes with Cobalt Homoenolates. Angew. Chem., Int. Ed 2021, 60, 2694–2698.(k)Nie S; Lu A; Kuker EL; Dong VM Enantioselective Hydrothiolation: Diverging Cyclopropenes through Ligand Control. J. Am. Chem. Soc 2021, 143, 6176–6184. [PubMed: 33856804] (l)Huang M-Y; Zhao Y-T; Chai H; Zhang C-D; Zhu S-F Copper-Catalyzed Ring-Opening/Borylation of Cyclopropenes. CCS Chem. 2022, 4, 1232–1237.(m)Yu R; Cai S; Li C; Fang X Nickel-Catalyzed Asymmetric

Hydroaryloxy- and Hydroalkoxycarbonylation of Cyclopropenes. Angew. Chem., Int. Ed 2022, 61, No. e202200733.(n)Huang Q; Chen Y; Zhou X; Dai L; Lu Y Nickel-Hydride-Catalyzed Diastereo- and Enantioselective Hydroalkylation of Cyclopropenes. Angew. Chem., Int. Ed 2022, 61, No. e202210560.

(13). For reviews, see:(a)Hirano K; Miura M Hydroamination, Aminoboration, and Carboamination with Electrophilic Amination Reagents: Umpolung-Enabled Regio- and Stereoselective Synthesis of N -Containing Molecules from Alkenes and Alkynes. J. Am. Chem. Soc 2022, 144, 648–661. [PubMed: 34986637] (b)Mohite SB; Bera M; Kumar V; Karpoormath R; Baba SB; Kumbhar AS O-Benzoylhydroxylamines: A Versatile Electrophilic Aminating Reagent for Transition Metal-Catalyzed C-N Bond-Forming Reactions. Top. Curr. Chem 2023, 381, 4.

(14). (a)Zhu S; Niljianskul N; Buchwald SL Enantio- and Regioselective CuH-Catalyzed Hydroamination of Alkenes. J. Am. Chem. Soc 2013, 135, 15746–15749. [PubMed: 24106781] (b)Miki Y; Hirano K; Satoh T; Miura M Copper-Catalyzed Intermolecular Regioselective Hydroamination of Styrenes with Polymethylhydrosiloxane and Hydroxylamines. Angew. Chem., Int. Ed 2013, 52, 10830–10834.(c)Liu RY; Buchwald SL CuH-Catalyzed Olefin Functionalization: From Hydroamination to Carbonyl Addition. Acc. Chem. Res 2020, 53, 1229–1243. [PubMed: 32401530]

(15). Paderes MC; Belding L; Fanovic B; Dudding T; Keister JB; Chemler SR Evidence for Alkene Cis-Aminocupration, an Aminooxygenation Case Study: Kinetics, EPR Spectroscopy, and DFT Calculations. Chem. - Eur. J 2012, 18, 1711–1726. [PubMed: 22237868]

(16). For selected examples of late-stage functionalization, see:(a)Wencel-Delord J; Glorius F C-H Bond Activation Enables the Rapid Construction and Late-Stage Diversification of Functional Molecules. Nat. Chem 2013, 5, 369–375. [PubMed: 23609086] (b)DiRocco DA; Dykstra K; Krska S; Vachal P; Conway DV; Tudge M Late-Stage Functionalization of Biologically Active Heterocycles Through Photoredox Catalysis. Angew. Chem., Int. Ed 2014, 53, 4802–4806.(c)Sharma A; Hartwig JF Metal-Catalyzed Azidation of Tertiary C-H Bonds Suitable for Late-Stage Functionalization. Nature 2015, 517, 600–604. [PubMed: 25631448] (d)Cernak T; Dykstra KD; Tyagarajan S; Vachal P; Krska SW The Medicinal Chemist's Toolbox for Late-Stage Functionalization of Drug-like Molecules. Chem. Soc. Rev 2016, 45, 546–576. [PubMed: 26507237] (e)Gianatassio R; Lopchuk JM; Wang J; Pan C-M; Malins LR; Prieto L; Brandt TA; Collins MR; Gallego GM; Sach NW; Spangler JE; Zhu H; Zhu J; Baran PS Strain-Release Amination. Science 2016, 351, 241–246. [PubMed: 26816372] (f)Shang M; Wang M; Saint-Denis TG; Li M; Dai H; Yu J Copper-Mediated Late-Stage Functionalization of Heterocycle-Containing Molecules. Angew. Chem., Int. Ed 2017, 56, 5317–5321.(g)Le C; Liang Y; Evans RW; Li X; MacMillan DWC Selective sp^3 C-H Alkylation via Polarity-Match-Based Cross-Coupling. Nature 2017, 547, 79–83. [PubMed: 28636596] (h)Uehling MR; King RP; Krska SW; Cernak T; Buchwald SL Pharmaceutical Diversification via Palladium Oxidative Addition Complexes. Science 2019, 363, 405–408. [PubMed: 30679373] (i)Feng K; Quevedo RE; Kohrt JT; Oderinde MS; Reilly U; White MC Late-Stage Oxidative C(sp3)-H Methylation. Nature 2020, 580, 621–627. [PubMed: 32179876] (j)Zhang L; Ritter T A Perspective on Late-Stage Aromatic C-H Bond Functionalization. J. Am. Chem. Soc 2022, 144, 2399–2414. [PubMed: 35084173]

(17). Trost B The Atom Economy A Search for Synthetic Efficiency. Science 1991, 254, 1471–1477. [PubMed: 1962206]

(18). For reviews, see:(a)Vicente, R. C-C Bond Cleavages of Cyclopropenes: Operating for Selective Ring-Opening Reactions. Chem. Rev 2021, 121, 162–226. [PubMed: 32639746] (b)Huo H; Gong Y Construction of Heterocyclic Rings from Cyclopropenes. Org. Biomol. Chem 2022, 20, 3847–3869. [PubMed: 35470816]

(19). For selected examples, see:(a)Lee EC; Fu GC Copper-Catalyzed Asymmetric N-H Insertion Reactions: Couplings of Diazo Compounds with Carbamates to Generate α-Amino Acids. J. Am. Chem. Soc 2007, 129, 12066–12067. [PubMed: 17877350] (b)Phan DTH; Dong VM Silver-Catalyzed Ring-Opening of Cyclopropenes: Preparation of Tertiary α-Branched Allylic Amines. Tetrahedron 2013, 69, 5726–5731.(c)Hyde S; Veliks J; Liégault B; Grassi D; Taillefer M; Gouverneur V Copper-Catalyzed Insertion into Heteroatom-Hydrogen Bonds with Trifluorodiazoalkanes. Angew. Chem., Int. Ed 2016, 55, 3785–3789.(d)Arredondo V; Hiew SC; Gutman ES; Premachandra IDUA; Van Vranken DL Enantioselective Palladium-Catalyzed

Carbene Insertion into the N-H Bonds of Aromatic Heterocycles. Angew. Chem., Int. Ed 2017, 56, 4156–4159.(e)Li M-L; Yu J-H; Li Y-H; Zhu S-F; Zhou Q-L Highly Enantioselective Carbene Insertion into N-H Bonds of Aliphatic Amines. Science 2019, 366, 990–994. [PubMed: 31753998]

(20). Muller P Glossary of Terms Used in Physical Organic Chemistry (IUPAC Recommendations 1994). Pure Appl. Chem 1994, 66, 1077–1184.

(21). For examples of regioselective functionalization of more sterically hindered pyrazole nitrogen, see:(a)Xu D; Frank L; Nguyen T; Stumpf A; Russell D; Angelaud R; Gosselin F Magnesium-Catalyzed N2-Regioselective Alkylation of 3-Substituted Pyrazoles. Synlett 2020, 31, 595–599. (b)Bengel LL; Aberle B; Egler-Kemmerer A; Kienzle S; Hauer B; Hammer SC Engineered Enzymes Enable Selective N-Alkylation of Pyrazoles with Simple Haloalkanes. Angew. Chem., Int. Ed 2021, 60, 5554–5560.(c)Chen S-J; Golden DL; Krska SW; Stahl SS Copper-Catalyzed Cross-Coupling of Benzylic C-H Bonds and Azoles with Controlled N-Site Selectivity. J. Am. Chem. Soc 2021, 143, 14438–14444. [PubMed: 34464528]

(22). For selected examples of regioselective functionalization of pyrazoles, see:(a)Antilla JC; Baskin JM; Barder TE; Buchwald SL Copper-Diamine-Catalyzed N -Arylation of Pyrroles, Pyrazoles, Indazoles, Imidazoles, and Triazoles. J. Org. Chem 2004, 69, 5578–5587. [PubMed: 15307726] (b)Goikhman R; Jacques TL; Sames D C-H Bonds as Ubiquitous Functionality: A General Approach to Complex Arylated Pyrazoles via Sequential Regioselective C -Arylation and N -Alkylation Enabled by SEM-Group Transposition. J. Am. Chem. Soc 2009, 131, 3042–3048. [PubMed: 19206533] (c)Ye Y; Kevlishvili I; Feng S; Liu P; Buchwald SL Highly Enantioselective Synthesis of Indazoles with a C3-Quaternary Chiral Center Using CuH Catalysis. J. Am. Chem. Soc 2020, 142, 10550–10556. [PubMed: 32408745] (d)Dow NW; Cabré A; MacMillan DWC A General N-Alkylation Platform via Copper Metallaphotoredox and Silyl Radical Activation of Alkyl Halides. Chem 2021, 7, 1827–1842. [PubMed: 34423174] (e)Das M; Zamani L; Bratcher C; Musacchio PZ Azolation of Benzylic C-H Bonds via Photoredox-Catalyzed Carbocation Generation. J. Am. Chem. Soc 2023, 145, 3861–3868.

(23). For reviews, see:(a)Singh J; Sharma D; Bansal R Pyridazinone: An Attractive Lead for Anti-Inflammatory and Analgesic Drug Discovery. Future Med. Chem 2017, 9, 95–127. [PubMed: 27957866] (b)Dubey S; Bhosle PA Pyridazinone: An Important Element of Pharmacophore Possessing Broad Spectrum of Activity. Med. Chem. Res 2015, 24, 3579–3598.

(24). For reviews, see:(a)Denya I; Malan SF; Joubert J Indazole Derivatives and Their Therapeutic Applications: A Patent Review (2013–2017). Expert Opin. Ther. Pat 2018, 28, 441–453. [PubMed: 29718740] (b)Mal S; Malik U; Mahapatra M; Mishra A; Pal D; Paidesetty SK A Review on Synthetic Strategy, Molecular Pharmacology of Indazole Derivatives, and Their Future Perspective. Drug Dev. Res 2022, 83, 1469–1504. [PubMed: 35971890]

(25). The low yields of **3s** and **3t** may arise from the electron deficiency of **2s** and **2t**.**3s3t2s2t**

(26). Zall CM; Linehan JC; Appel AM Triphosphine-Ligated Copper Hydrides for CO_2 Hydrogenation: Structure, Reactivity, and Thermodynamic Studies. J. Am. Chem. Soc 2016, 138, 9968–9977. [PubMed: 27434540]

(27). For a given species A, VTNA experiments are conducted by plotting the product formation against time normalized to various orders of [A] (0, 1, 2, fractional, etc.). Overlays are attained when the assumed order is accurate. For more details, see the SI and:Burés J Variable Time Normalization Analysis: General Graphical Elucidation of Reaction Orders from Concentration Profiles. Angew. Chem., Int. Ed 2016, 55, 16084–16087.

(28). (a)Yang X-H; Davison RT; Dong VM Catalytic Hydrothiolation: Regio- and Enantioselective Coupling of Thiols and Dienes. J. Am. Chem. Soc 2018, 140, 10443–10446. [PubMed: 30091909] (b)Yang X-H; Davison RT; Nie S-Z; Cruz FA; McGinnis TM; Dong VM Catalytic Hydrothiolation: Counterion-Controlled Regioselectivity. J. Am. Chem. Soc 2019, 141, 3006–3013. [PubMed: 30735362]

(29). (a)Rosner T; Le Bars J; Pfaltz A; Blackmond DG Kinetic Studies of Heck Coupling Reactions Using Palladacycle Catalysts: Experimental and Kinetic Modeling of the Role of Dimer Species. J. Am. Chem. Soc 2001, 123, 1848–1855. [PubMed: 11456804] (b)Burés J A Simple Graphical Method to Determine the Order in Catalyst. Angew. Chem., Int. Ed 2016, 55, 2028–2031.

(30). For examples of off-cycle catalysts, see:(a)Hein JE; Armstrong A; Blackmond DG Kinetic Profiling of Prolinate-Catalyzed α-Amination of Aldehydes. Org. Lett 2011, 13, 4300–4303. [PubMed: 21761822] (b)Bandar JS; Pirnot MT; Buchwald SL Mechanistic Studies Lead to Dramati cally Improved Reaction Conditions for the Cu-Catalyzed Asymmetric Hydroamination of Olefins. J. Am. Chem. Soc 2015, 137, 14812–14818. [PubMed: 26522837] (c)Blackmond DG Kinetic Profiling of Catalytic Organic Reactions as a Mechanistic Tool. J. Am. Chem. Soc 2015, 137, 10852–10866. [PubMed: 26285166]

(31). Gibbons SK; Valleau CRD; Peltier JL; Cain MF; Hughes RP; Glueck DS; Golen JA; Rheingold AL Diastereoselective Coordination of P-Stereogenic Secondary Phosphines in Copper(I) Chiral Bis(Phosphine) Complexes: Structure, Dynamics, and Generation of Phosphido Complexes. Inorg. Chem 2019, 58, 8854–8865. [PubMed: 31247872]

(32). For examples, see:(a)Titov AA; Filippov OA; Smol'yakov AF; Baranova KF; Titova EM; Averin AA; Shubina ES Dinuclear Cu^I and Ag^I Pyrazolates Supported with Tertiary Phosphines: Synthesis, Structures, and Photophysical Properties. Eur. J. Inorg. Chem 2019, 2019, 821–827. (b)Watanabe Y; Washer BM; Zeller M; Savikhin S; Slipchenko LV; Wei A Copper(I)-Pyrazolate Complexes as Solid-State Phosphors: Deep-Blue Emission through a Remote Steric Effect. J. Am. Chem. Soc 2022, 144, 10186–10192. [PubMed: 35594145]

(33). Luo Y; Hou Z A Five-Center Rather than a Four-Center Transition State for Alkene Insertion into the Metal-Alkyl Bond of a Cationic Binuclear Yttrium Complex. Organometallics 2006, 25, 6162–6165.

(34). Zhao Y; Truhlar DG The M06 suite of density functionals for main group thermochemistry, thermochemical kinetics, non-covalent interactions, excited states, and transition elements: two new functionals and systematic testing of four M06-class functionals and 12 other functionals. Theor. Chem. Acc 2008, 120, 215–241.

(35). Hehre WJ; Stewart RF; Pople JA Self-Consistent Molecular-Orbital Methods. I. Use of Gaussian Expansions of Slater-Type Atomic Orbitals. J. Chem. Phys 1969, 51, 2657–2664.

(36). Validation of the five-centered aminocupration transition state (TSCA-N2) was achieved by locating the corresponding transition state at both the ωB97XD/def2-TZVP PCM(MeCN)//B97D/def2-SVP and B3LYP-D3BJ/6–311+G** PCM(MeCN)//B3LYP-D3BJ/6–31G* levels of theory.

(37). Frisch MJ; Trucks GW; Schlegel HB; Scuseria GE; Robb MA; Cheeseman JR; Scalmani G; Barone V; Petersson GA; Nakatsuji H; Li X; Caricato M; Marenich A; Bloino J; Janesko BG; Gomperts R; Mennucci B; Hratchian HP; Ortiz JV; Izmaylov AF; Sonnenberg JL; Williams-Young D; Ding F; Lipparini F; Egidi F; Goings J; Peng B; Petrone A; Henderson T; Ranasinghe D; Zakrzewski VG; Gao J; Rega N; Zheng G; Liang W; Hada M; Ehara M; Toyota K; Fukuda R; Hasegawa J; Ishida M; Nakajima T; Honda Y; Kitao O; Nakai H; Vreven T; Throssell K; Montgomery JA Jr.; Peralta JE; Ogliaro F; Bearpark M; Heyd JJ; Brothers EN; Kudin KN; Staroverov VN; Keith TA; Kobayashi R; Normand J; Raghavachari K; Rendell AP; Burant JC; Iyengar SS; Tomasi J; Cossi M; Millam JM; Klene M; Adamo C; Cammi R; Ochterski JW; Martin RL; Morokuma K; Farkas O; Foresman JB; Fox DJ Gaussian 16, rev. C.01; Gaussian, Inc.: Wallingford, CT, 2016.
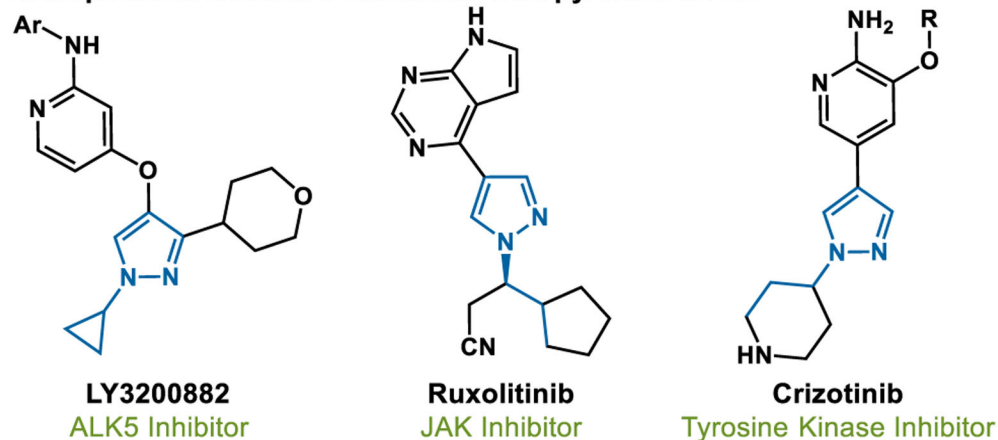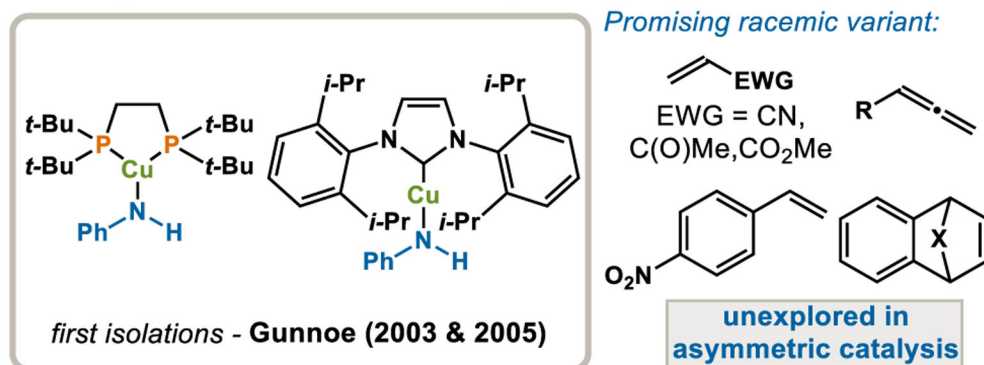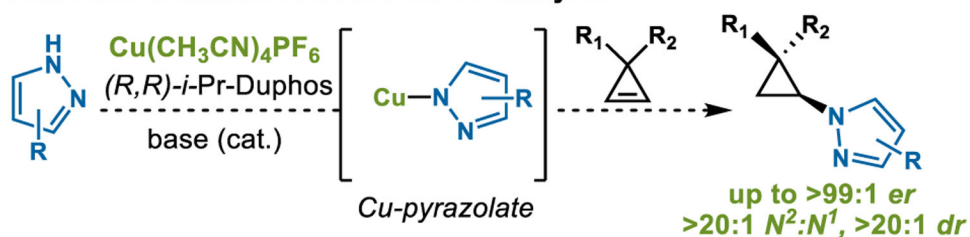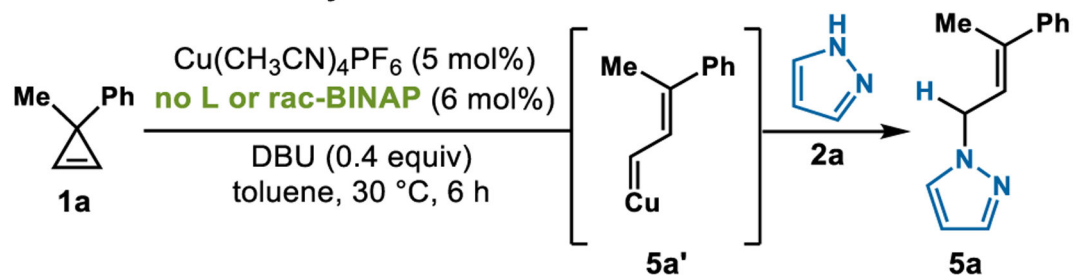
Figure 1.
Asymmetric hydroamination of cyclopropenes with pyrazoles.

A. Undesired reactivity identified

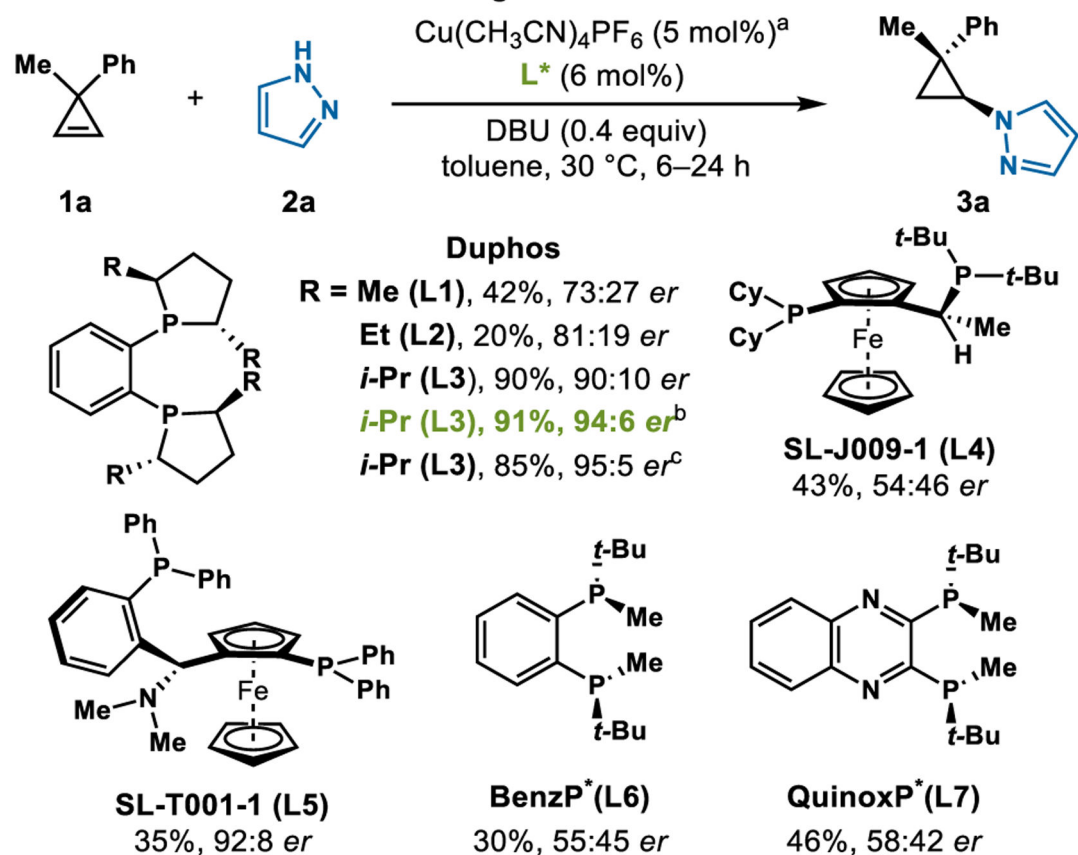## B. Effect of electron-rich chiral ligands

Duphos

R = Me (L1), 42%, 73:27 *er*
Et (L2), 20%, 81:19 *er*
i-Pr (L3), 90%, 90:10 *er*
i-Pr (L3), 91%, 94:6 *er*[b]
i-Pr (L3), 85%, 95:5 *er*[c]

SL-J009-1 (L4)
43%, 54:46 *er*

SL-T001-1 (L5)
35%, 92:8 *er*

BenzP*(L6)
30%, 55:45 *er*

QuinoxP*(L7)
46%, 58:42 *er*

Figure 2.
Reaction optimization using bisphosphine ligands. [a]Reaction conditions: **1a** (0.12 mmol), **2** (0.10 mmol), Cu(CH$_3$CN)$_4$PF$_6$ (5 mol%), chiral ligand (6 mol%), toluene (0.4 mL), 30 °C, 6–24 h. Yields of isolated products are given. Enantiomeric ratios (*er*) were determined by SFC analysis on a chiral stationary phase. [b]The reaction was performed using CH$_3$CN at 30 °C for 6 h. [c]The reaction was performed using CH$_3$CN at 0 °C for 4 days.
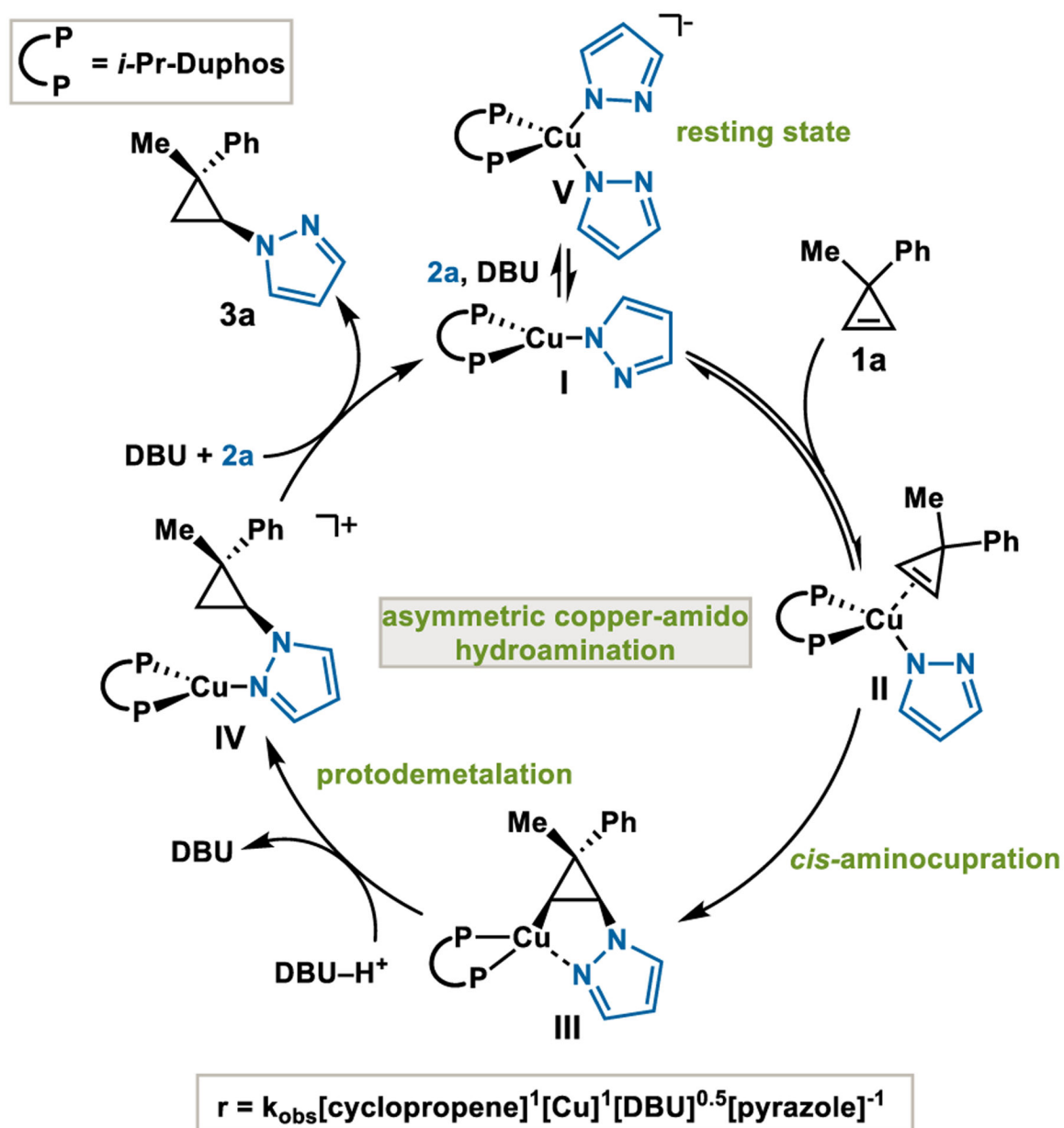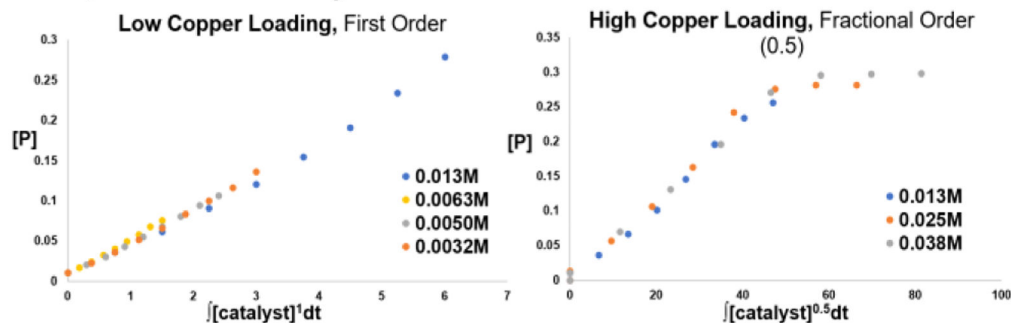
Figure 3.
Proposed catalytic cycle.

A. Dependence of catalyst order on concentration

Low Copper Loading, First Order

[P]

- 0.013M
- 0.0063M
- 0.0050M
- 0.0032M

∫[catalyst]¹dt

High Copper Loading, Fractional Order (0.5)

[P]

- 0.013M
- 0.025M
- 0.038M

∫[catalyst]$^{0.5}$dt

B. Attempt to probe the resting state

VI

$\binom{P}{P}$ = *i*-Pr-Duphos

≡ [X-Ray]

Me, Ph + pyrazole(N-H) →

"**Cu-trimer VI**" (5 mol%)
DBU (0.4 equiv)

CH$_3$CN, 30 °C, 12 h
20% yield, 94:6 *er*

Me, Ph (cyclopropane-pyrazole product)
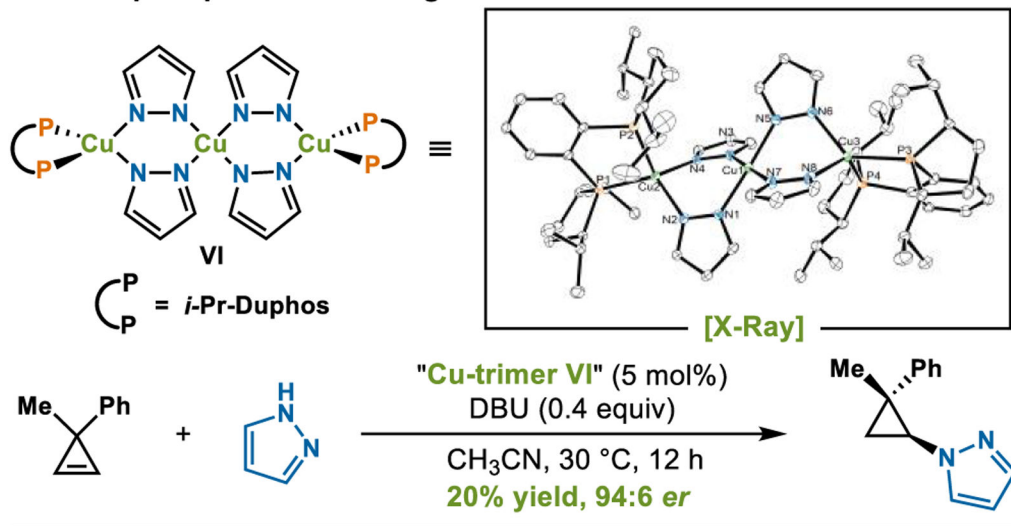
C. Deuterium labeling study

Me, Ph (cyclopropene, D) + 2q (indazole N-H) →

Cu(CH$_3$CN)$_4$PF$_6$ (5 mol%)
L3 (6 mol%)

DBU (0.4 equiv)
CH$_3$CN, 60 °C

→ Me, Ph, H, D, D product

d-**1a**   **2q**
75% D%

d-**3q**
72% *cis*-H
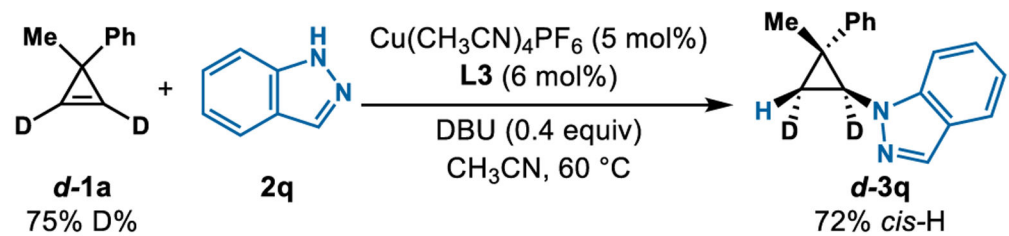
Figure 4.
Mechanistic studies.
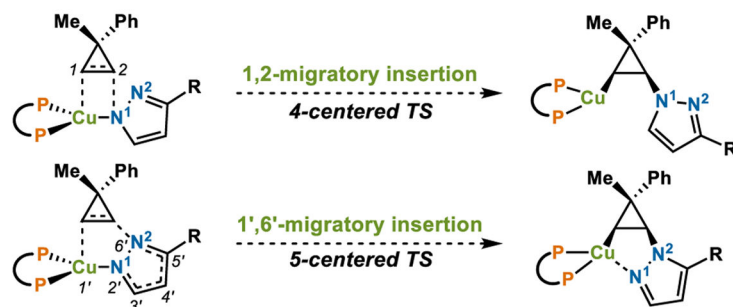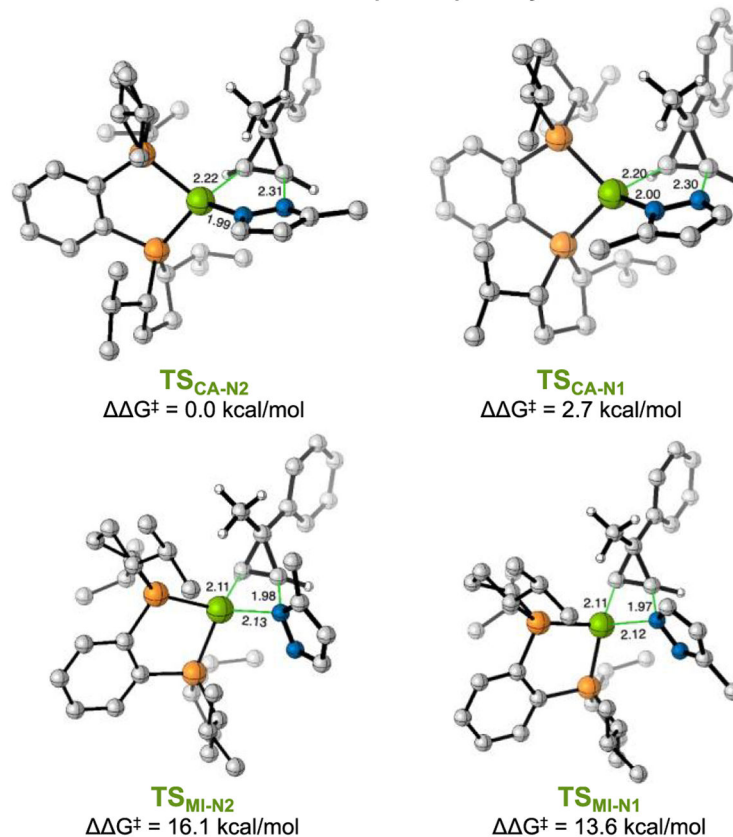
Figure 5.
Proposed C–N bond formation pathways and TSs for the favored five-centered $1',6'$-migratory insertion of N^2 (**TS**$_{CA-N2}$) and the higher energy, disfavored four-centered 1,2-migratory insertion of N2 (**TS**$_{MI-N2}$).

Table 1.

Scope of Pyrazoles and Other N-Heterocycles.
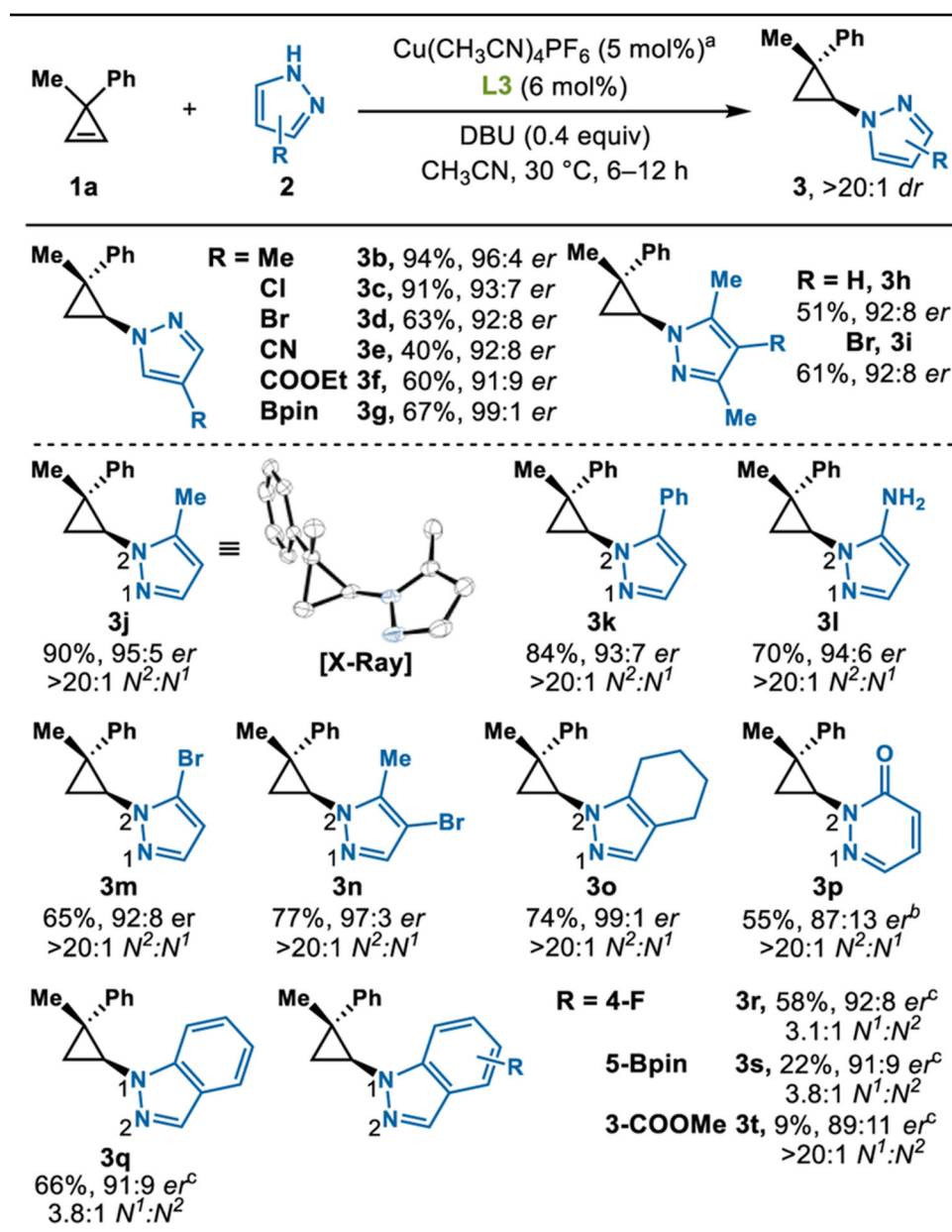
Reaction scheme:

1a + **2** → Cu(CH₃CN)₄PF₆ (5 mol%)ᵃ, L3 (6 mol%), DBU (0.4 equiv), CH₃CN, 30 °C, 6–12 h → **3**, >20:1 *dr*

R = Me, **3b**, 94%, 96:4 *er*
Cl, **3c**, 91%, 93:7 *er*
Br, **3d**, 63%, 92:8 *er*
CN, **3e**, 40%, 92:8 *er*
COOEt **3f**, 60%, 91:9 *er*
Bpin **3g**, 67%, 99:1 *er*

R = H, **3h** 51%, 92:8 *er*
Br, **3i** 61%, 92:8 *er*

3j 90%, 95:5 *er* >20:1 N²:N¹ [X-Ray]

3k 84%, 93:7 *er* >20:1 N²:N¹

3l 70%, 94:6 *er* >20:1 N²:N¹

3m 65%, 92:8 *er* >20:1 N²:N¹

3n 77%, 97:3 *er* >20:1 N²:N¹

3o 74%, 99:1 *er* >20:1 N²:N¹

3p 55%, 87:13 *er*ᵇ >20:1 N²:N¹

3q 66%, 91:9 *er*ᶜ 3.8:1 N¹:N²

R = 4-F **3r**, 58%, 92:8 *er*ᶜ 3.1:1 N¹:N²
5-Bpin **3s**, 22%, 91:9 *er*ᶜ 3.8:1 N¹:N²
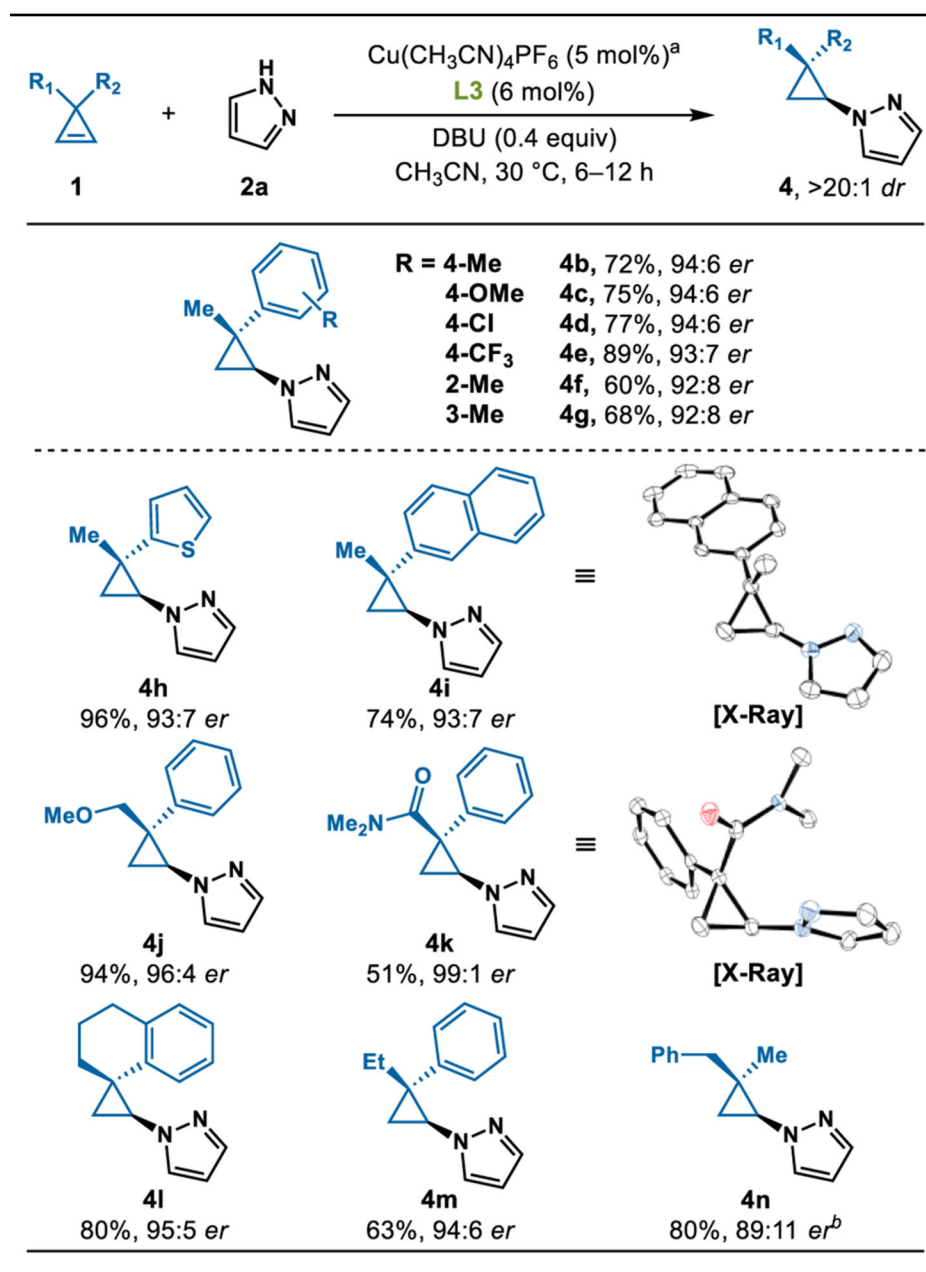3-COOMe **3t**, 9%, 89:11 *er*ᶜ >20:1 N¹:N²

[a] Reaction conditions: **1a** (0.12 mmol), **2** (0.10 mmol), Cu(CH₃CN)₄PF₆ (5 mol%), L3 (6 mol%), CH₃CN (0.4 mL), 30 °C, 6–12 h. Yields of isolated products are given. Nitrogen regioisomeric ratios (N²:N¹) were determined based on isolated yields and NOE experiments. Diastereomeric ratios (*dr*) were determined from ¹H NMR analysis of the reaction mixtures. Enantiomeric ratios (*er*) were determined by SFC analysis on a chiral stationary phase.

[b] 24 h.

[c] The reaction was performed at 60 °C.

Table 2.

Scope of Cyclopropenes

Cu(CH₃CN)₄PF₆ (5 mol%)[a]
L3 (6 mol%)
DBU (0.4 equiv)
CH₃CN, 30 °C, 6–12 h

4, >20:1 *dr*

R =		
4-Me	**4b,** 72%, 94:6 *er*	
4-OMe	**4c,** 75%, 94:6 *er*	
4-Cl	**4d,** 77%, 94:6 *er*	
4-CF₃	**4e,** 89%, 93:7 *er*	
2-Me	**4f,** 60%, 92:8 *er*	
3-Me	**4g,** 68%, 92:8 *er*	

4h
96%, 93:7 *er*

4i
74%, 93:7 *er*

[X-Ray]

4j
94%, 96:4 *er*

4k
51%, 99:1 *er*

[X-Ray]

4l
80%, 95:5 *er*

4m
63%, 94:6 *er*

4n
80%, 89:11 *er*[b]

[a] Reaction conditions: **1** (0.12 mmol), **2a** (0.10 mmol), Cu(CH₃CN)₄PF₆ (5 mol%), **L3** (6 mol%), CH₃CN (0.4 mL), 30 °C, 6–12 h. Yields of isolated products are given. Diastereomeric ratios (*dr*) were determined from ¹H NMR analysis of the unpurified reaction mixtures. Enantiomeric ratios (*er*) were determined by SFC analysis on a chiral stationary phase.

[b] 1:1 *dr.*